

HDL: A Novel Hydrology Defined Loss Function for Enhanced Physics based deep learning for crop yield prediction

Sakshi Gandotra¹, Rita Chhikara¹, Anuradha Dhull¹

¹The NorthCap University, Gurugram

ARTICLE INFO

Received: 29 Dec 2024

Revised: 15 Feb 2025

Accepted: 24 Feb 2025

ABSTRACT

Introduction-Agronomy is multi-dimensional and complex by nature. Agricultural prediction problems, especially yield prediction, exist in a universe of uncertainty since the highly non-linear and heterogeneous set of determinants exists. Although deep learning methods have been tried for yield prediction, their performance is constrained by spatial granularity issues and not using enough domain knowledge.

Objectives-This paper responds to the questions raised earlier by highlighting two critical issues in making precise predictions of yield using deep learning models.

Method-The research provides a CNN-LSTM model for rice yield prediction with emphasis on block level (administrative unit of state) spatial resolution for the Jammu district. While attempting to improve the accuracy of prediction, the research includes a physics-guided, hydrology-based loss function for the CNN-LSTM model.

Results-The results validate that the new loss function has made improved prediction compared to the baseline deep learning architectures of CNN, LSTM, and the basic CNN-LSTM.

Conclusion-The incorporation of a physics-informed, hydrology-sourced loss function into a CNN-LSTM model considerably alleviates issues of spatio-temporal variations and lack of integration of domain knowledge, resulting in improved predictions of rice yield.

Keywords: Physics Defined Neural Networks, Deep Learning, CNN-LSTM , Soil water balance equation, NDVI, NDMI, Crop Yield Prediction

INTRODUCTION

History of agriculture predictive Analytics

Predictive analytics in agriculture can be traced back to the 1800s when farmers started creating records of their yields and weather patterns. In the 1930s, statistical analysis became more standard, and more advanced predictive analytics soon followed (Figure 1). With technological advancements, farmers can collect and analyze data more efficiently, improving agricultural practices.

The benefits of predictive analytics in agriculture are vast. **Farmers use it to optimise crop yield and minimize damage from pests and diseases. It helps farmers make informed irrigation decisions, reducing water waste and higher crop yields. Farmers can save costs on resources, such as fertilisers, by accurately predicting outcomes and increasing their profits.**

Predictive analytics also helps farmers stay ahead of the curve. With predictions of weather patterns and the commodity market, farmers can plan their crops accordingly and make appropriate decisions to minimize the risk of crop loss or loss of margin. They are saving time and resources and improving their overall efficiency. Predictive analytics is a powerful tool for shaping farming practices and disrupting established procedures and protocols. And yet, it's not a new tool – the history of predictive analytics in agriculture goes back decades. It's just that today we have more data, better data, and better technology to analyze the data. The benefits of predictive analytics are enormous. Change can happen faster than it has in decades past. Predictive analytics is shaping to become a vital tool for farmers worldwide.

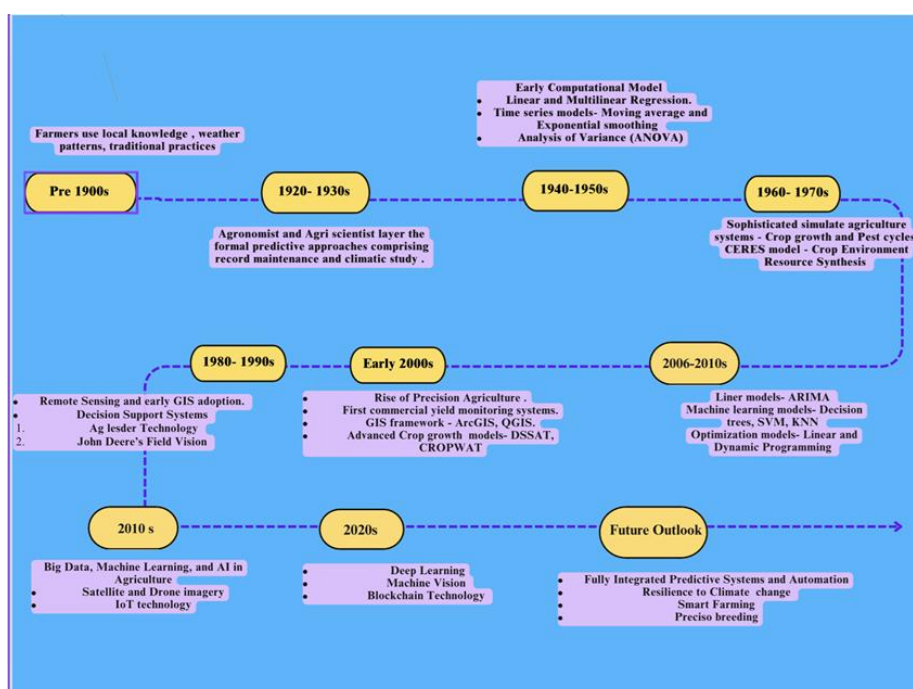


Figure 1-Depicts chronological evolution of how statistical agricultural tools have served the agriculture industry

Resurging interest in machine learning is due to the same factors that have made data mining and Bayesian analysis more popular than ever. Things like growing volumes and varieties of available data, computational processing that is cheaper and more powerful, affordable data storage. Machine learning (ML) is increasingly seen as the **future step** for predictive analytics in agriculture because of its ability to handle complex, non-linear relationships within large datasets, and its capacity to continuously learn and improve from new data. The agriculture sector faces a host of unpredictable variables, including weather conditions, pests, soil health, and market fluctuations. Traditional methods of predictive analytics, while useful, often fall short in terms of accuracy and scalability when it comes to complex agricultural systems. That's why machine learning is poised to revolutionise predictive analytics in agriculture. Farmers are empowered and can leverage these technologies to make data-driven choices for maximum efficiency and profitability, optimise planting schedules, predict disease outbreaks, and automate decision-making processes. Machine learning powered agriculture analytics systems offer recommendations for resource allocation, yield predictions, crop selection, and pest management.

Crop yield based predictions are needed to improve the food security, enhanced the farm management, make informed decisions, manage financial risk margins, make informed market forecasting, optimise the supply demand management and can relate effects of climate change effectively. crop yield prediction analytics helps to reflect the business domain situation for seed businesses, food-based companies and retailing commodity traders.

In last decade ML practitioners have shifted from classic ML models and LR methods [Nevavouri, Becker Reshef, Kang, Wang, adaboost] to DNN based yield predictions due to the intrinsic ability of NN to capture fine non linear relationships. [Wang, Sun]. Authors have attempted to include effect of neighbouring water bodies and urban built up. [sagarika]. With more advanced satellite images, Qiao, Gavahi has attempted to provide 3D CNN based yield predictions.

Despite all the above efforts, Neural networks are generally incapable of generalising what they learn from a data set. As a result, they often struggle to make consistent or accurate predictions outside the data domain in which they were trained. This becomes especially problematic when working with dynamic systems where small changes in the data relationships can lead to large-scale distribution changes. Expert knowledge of the system can provide a basis for neural networks to extrapolate to new scenarios, allowing them to make more effective generalisation. Physics-based machine learning (PBML) can outperform traditional machine learning (ML)-based crop yield predictions in certain

scenarios because it incorporates the principles of physics and domain-specific knowledge about natural systems into the model. crop yield is influenced by weather, soil composition, water availability, plant physiology, etc. A physics-based model can explicitly incorporate these constraints (like conservation of mass and energy, water flow, photosynthesis dynamics, etc.) to provide a more grounded prediction.[He, Liu, Jia, Doaa].

MOTIVATION

- a. Broad spatial resolution crop yield predictions, such as those at district or regional levels, often miss localised variations in environmental conditions, soil types, and farming practices. Machine learning models for crop yield prediction typically rely on lower-resolution datasets due to the scarcity of high-resolution data. This challenge is particularly evident in the Indian subcontinent, where most yield prediction studies focus on the district level, with some extending to the tehsil level. Given that the majority of Indian farmers operate on very small landholdings, the need for precise technological interventions is critical. As shown in Fig, the performance of deep learning models declines with the lack of fine spatial granularity in yield predictions. This highlights the urgent need for research to shift towards finer scales, especially at the panchayat samiti level, to capture more localised insights that can support targeted interventions and optimise resource. (Figure 2).

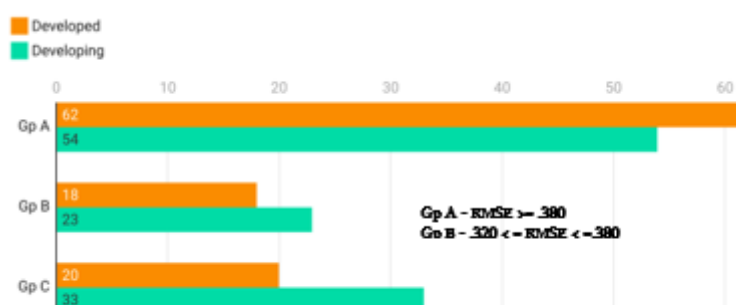


Figure 2 - Graph showing impact of spatial granularity of yield predictions on RMSE for respective number of research papers.

Coupling of hydrologic principle allows physically consistent and interpretable model

Physical processes, such as the movement of water through the soil, nutrient uptake by plants, and the relationship between solar radiation and photosynthesis, follow well-understood laws. By including these in the model, physics-based machine learning can offer more robust predictions. The Soil Water Balance (SWB) equation [Slatyer, 1962] is the foundation of nearly all soil water behavior in the root zone as a driving force of actual evapotranspiration and thereby biomass development and yield formation in crops.

The yield of rice, which is highly sensitive to water availability, effectively referenced using the **soil water balance equation**. This approach helps in understanding how different components of the water cycle (like rainfall, irrigation, evapotranspiration, runoff, and deep percolation) impact the water available to rice plants and, consequently, their growth and yield (Figure 3). As the crop grows and extracts water from the soil to satisfy its ET_c requirement, the stored soil water is gradually depleted. In general, the net irrigation requirement is the amount of water required to refill the root zone soil water content back up to field capacity. This amount, which is the difference between field capacity and current soil water level, corresponds to the soil water deficit (D). On a daily basis, D can be estimated using the following accounting equation for the soil root zone:

$$WY = P + ET_c - R \quad (1)$$

Model Preliminaries

Research Article

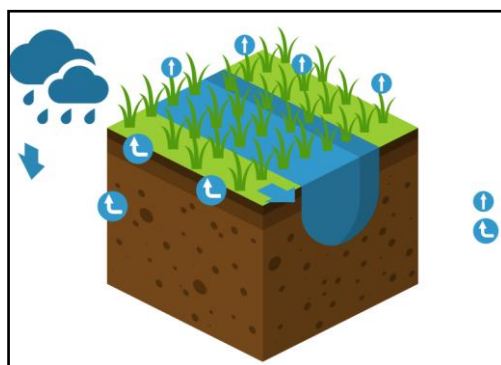


Figure 3 -Soil water balance phenomena

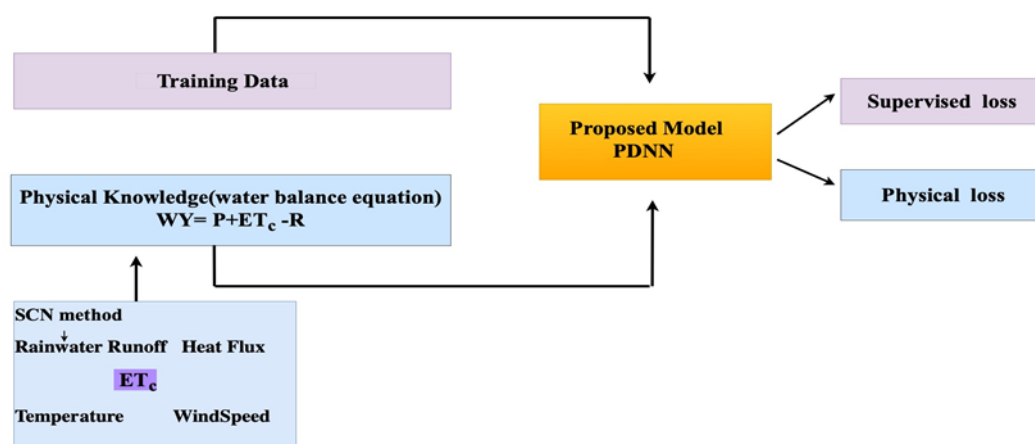


Figure 4 – The flow mechanism of the proposed PDNN model .

LITERATURE REVIEW

The application of machine learning, specifically deep neural networks (DNNs) and satellite-based phenology data, in crop yield prediction has been convincingly established by studies like [Sharma et al 2020], [Sun et al. 2019], and [Jiang et al 2019]. Evidence for this is the development of Convolutional Neural Networks (CNNs) as high-dimensional forms, described by [Pothapragada et al. 2025], [Wang et al. 2020], which transformed feature extraction of spectral information from Multi-Spectral Imaging (MSI) data to enable further investigation of complex agricultural landscapes.

Recently developed Physics-Informed Neural Networks (PINNs) deep learning models are a result of integrating low level physical knowledge into the system's architecture, as domain specific information fusion emerged as a significant concern within artificial intelligence. Such integration has been pioneered by Raissi et al. [2019], who developed a framework for incorporating physical considerations into neural networks by using them to solve partial differential equations, demonstrating success when the physical laws of the problem were defined within the loss function of the neural network's framework. This idea has been adopted for a multitude of environmental and earth system modeling attempts [Willard et al., 2020; Irrgang et al., 2021] where data is scarce and models need to be more robust and interpretable. He et al. introduced the Physics-Guided Attention Network (PG-AN), which uses physical knowledge from existing models to enhance feature extraction and identify distribution shifts over time. The model then uses these physics-informed embeddings to adjust training samples, refining the PG-AN model to align more closely with target year distributions. In agriculture, physical laws such as those relating to the water balance of soil, plant physiology, and energy exchange are being used to design constraints and guide deep learning models to more optimal solutions [e.g., Zhao et al. 2019 & Liu et al. 2023]. The results of this inter-disciplinary research approach do not only provide accurate data but also produce reasoning that stands the test of interpretation which strengthens

the reliability of crop yield forecasting tools considering the changing environment. Table 1 delineates brief of research studies conducted in domain guided emerging field of deep learning.

Even though these developments seem to hold major potential, the highlighted gaps in interpretability, generalizability, and spatial accuracy resolution for more complex settings such as India persist. Table 2 summarises deep learning based crop yield prediction models developed for Indian Landscape. To address these gaps, this paper presents a new crop yield prediction model based on Physics-Driven Deep Neural Network (PDNN) which incorporates a Soil Water Balance (SWB) equation framework into its loss function. This approach delivers predictions at the domain level by incorporating priors into the integrated CNN-LSTM model, optimizing accuracy while maintaining physical consistency and driving better spatio-temporal feature extraction than methods which rely on data alone.

Table 1. Description of Physics incorporated Seminal deep learning studies

Paper	ML model	Characteristics	Application	Crop	RMSE
Kallenberg et al.	CNN	Synthetic data from TIPSTAR	CYP	Potato	.362
Pylaniadis et al.	Random Forest	Uses data generated from APSIM	Nitrogen response prediction	Green pasture	.354
Shahhosseini et al.	Extreme Gradient Boost Light GBM, Lasso, Random Forest	APSIM integration with ML models	CYP	Corn	.420
Han et al.	LSTM	Uses ORYZA to design output layer of LSTM	CYP	Rice	.370
McCormick et al.	LSTM	Couples phenology models of CROPGRO with CNN	Phenology prediction	Soybean	.351
Worrall et al.	LSTM	Builds branched LSTM structure based on eco physical relation	Prediction of corn growth phases	Corn	.382
He et al.	Attention based LSTM	Uses Mass Carbon Conservation equation for physical penalty	CYP	Corn and Wheat	.366
Maulana et al.		Uses TIPSTAR potato model in ML model of SINDI- PY using switching technique	CYP	Potato	.371

In particular, the proposed Physics Derived Neural Network (PDNN) regresses key variables involved in water balance equation with the constraint of water yield. Further, With meteorology and phenology data as input vector, the proposed model uses rice yield data over six blocks of Jammu district over the time period of 2014-2019. Outline of the paper presented has been given in figure 5.



Figure 5 .Outline of the Paper.

DATA SET AND MATERIAL

Dataset

Satellite Imagery

The satellite images used in this study were obtained from Landsat and Sentinel-2A satellites, covering the periods from 2014 to 2016 and 2017 to 2019, respectively. The study employs phenological features such as the Normalized Difference Vegetation Index (NDVI) and the Normalized Difference Moisture Index (NDMI) to assess the biomass and water content of rice crops (see Fig. 12). Equipped with a multispectral imaging instrument (MSI), these satellites capture data across various electromagnetic (EM) spectral bands, providing NDVI and NDMI data alongside true colour images of the target area. Table III outlines the characteristics of these satellite-sourced indices.

NDVI (Normalized Difference Vegetation Index)

NDVI measures the health of green foliage by analysing the normalized scattering of Near Infrared (NIR) wavelengths and chlorophyll absorption in red wavelengths. It assesses photosynthetically active biomass, where healthy crops absorb most visible wavelengths and reflect a large proportion of NIR light. Landsat and Sentinel-2A satellite images, captured during 2014-2016 and 2017-2019, are used for this analysis. The Sentinel-2 satellites, including both Sentinel-2A and 2B, are equipped with an MSI covering 13 spectral bands (443–2190 nm), with a swath width of 290 km and spatial resolutions of 10 m (four visible and near-infrared bands), 20 m (six red edge and shortwave infrared bands), and 60 m (three atmospheric correction bands) [see Table 4 (a to b)]. The NDVI ratio for Sentinel-2 is calculated using Band 8 (865 nm) and Band 4 (665 nm) as per Equation (6). Healthy vegetation typically absorbs most visible light and reflects a high proportion of NIR light, whereas areas with poor vegetation or sparse coverage exhibit the opposite pattern.

****NDMI (Normalized Difference Moisture Index) ****

NDMI is used to monitor changes in foliage moisture levels by analysing both Near Infrared (NIR) and Short-Wave Infrared (SWIR) reflectance. The SWIR band measures water content in vegetation and the spongy mesophyll structure within canopies, while the NIR reflectance is influenced by leaf internal structure and dry matter content, excluding water content. By combining NIR and SWIR data, NDMI eliminates variations caused by internal leaf structure and dry matter content, improving moisture level precision. The NDMI ratio for Sentinel-2 is computed using Band 8 (865 nm) and Band 11 (1610 nm) according to Equation (7).

$$NDMI = (NIR - SWIR) / (NIR + SWIR) \quad (7)$$

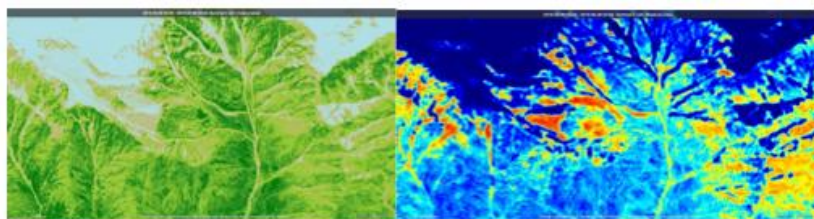


Figure 6. NDVI and NDMI imagery for tillering stage of rice crop (Location-block R.S Pura, date 06-05-2019, satellite: Sentinel 2A)

Table III. Description of satellite sourced phenology features.

Variable name	Description	Bands	Spatial resolution	Temporal resolution	Satellite
NDVI (Normalised difference Vegetation Index)	-1.0 to +1.0	NIR and Red	300 m	8 - Day composite	Landsat - 2014-2016 Sentinel 2A- 2017-2019
NDMI (Normalised Difference Moisture Index)	-1.0 to +1.0	NIR and SWIR	300 m	8 - Day composite	Landsat - 2014-2016 Sentinel 2A- 2017-2019

(a)					(b)				
Electromagnetic band	Nomenclature	Central wavelength	Bandwidth	Resolution	Dates of satellite image acquisition Period: 2014- 2019				
Red	B04	665 nm	30nm	10 m/pixel	12/5,18/5,25/5,30/5,6/6,11/6,16/6,22/6,28/6,5/7,10/7,15/7,20/7,25/7,1/8,0/8,25/8,30/8,5/9,10/9,15/9,20/9,25/9,30/9,5/10,15/10,15/10,20/10,25/10,5/11,10/11,15,11				
NIR- Near Infrared	B08A	865 nm	20nm	20 m/pixel					
SWIR- Shortwave Infrared	B11	1610 nm	90nm	20 m/pixel					
(c)					(d)				
Image resolution	Resolution of X axis (m/px)		Resolution of Y axis (m/px)		Block	Latitude,Longitude			
1571 x 898 pixel	2 meter / pixel		2 meter / pixel		Akhnoor	32.8969° N, 74.7354° E			
					Bishnah	32.6108° N, 74.8595° E			
					Bhalwal	32.2751° N, 72.9047° E			
					Marh	32.8946° N, 74.8361° E			
					Nagrota	32.7983° N, 74.9152° E			
					R.S Pura	32.6049° N, 74.7315° E			

Table 4. (a) Description of EM wavelengths used for NDMI and NDWI.(b) The calendar dates of acquired satellite images. (c) Resolution of satellite image .(d) Map coordinates for blocks (panchayat samitis)

Meteorology data

Crop-specific yield data were obtained from the Directorate of Agriculture in Jammu for the period 2014-2019. Weather data was compiled from the Agro-meteorology department of SKAUST, Jammu (Sher-e-Kashmir Agricultural University of Science and Technology). The variables are used with temporal aggregation of 1-day - temperature, rainfall, basic sunshine hours, humidity and solar radiation are summarised in Table V.

Table V. Description of Meteorology features.

Variable name	Unit	Range
Max (T), Maxim	°C	Max(T) - 6.5°C to 44.8°C

um Temperature		
Min (T)- minimum Temperature	°C	Min(T)- 0.0 °C to 3.0°C
RH(M) - Relative Humidity (Morning)	%	RH(M) -0.4 to 29.1
RH(E) - Relative Humidity (Evening)		RH(E)- 0.4 to 95.0
SR (Solar Radiation)	MJ/ day	3.3 to 64.9
RF (Rainfal l)	m m	0 to 25.3
BSSH (Basic Sunshine hours)	Hr s.	0 to 12.4

Yield Data

Panchayats Sammiti -level rice yield data from 2014 to 2019 was procured from the directorate of Agriculture, J&K. The unit of the yield scalar is quintals per hectare.

PROPOSED MODEL

The objective of the study is to build the physics derived deep learning model for the prediction of rice yield of respective block of Jammu district . The framework comprises two main components, a physical process model and a neural network. Then Neural part is : CNN followed by LSTM.

Physical process included is water balance phenomena. Two parts of physical process usage :

1. What phenomena ?
2. How it is employed in deep learning model ?

Proposed deep learning model has two machine learning components to achieve spatio them; oral feature extraction.– CNN and LSTM. Convolutional Neural Network (CNN) for feature extraction and a Long Short-Term Memory (LSTM) network for temporal feature learning.

2D CNN- ConvNet 2D-1 comprises of 4-layer .The initial three layers consist of the concatenation of convolution and pooling with 8, 16 and 32 number of filters respectively. The number of filters is doubled with each subsequent convolutional layer to increase the number of feature maps in the hidden layers. A small kernel size of 3×3 is used to represent the multi-level features. The rectified nonlinear activation function (ReLU) is performed after every convolution to introduce non-linearity to the CNN and is followed by the batch normalisation layer. Then a max-

pooling layer follows with size 2×2 and stride 2 that down samples the spatial dimension of the input and reduces the computational burden. In the last layer i.e., the FC layer, each neuron provides a full connection to all the learned feature maps issued from the previous layers. The fully connected layer together with a softmax activation at the end uses learned high-level features of the input images.

LSTM is used for sequential learning, with two layers of 100 hidden units each, corresponding to six-time steps of the crop season. Adam optimizer with a learning rate of 0.001 is used for network optimisation.

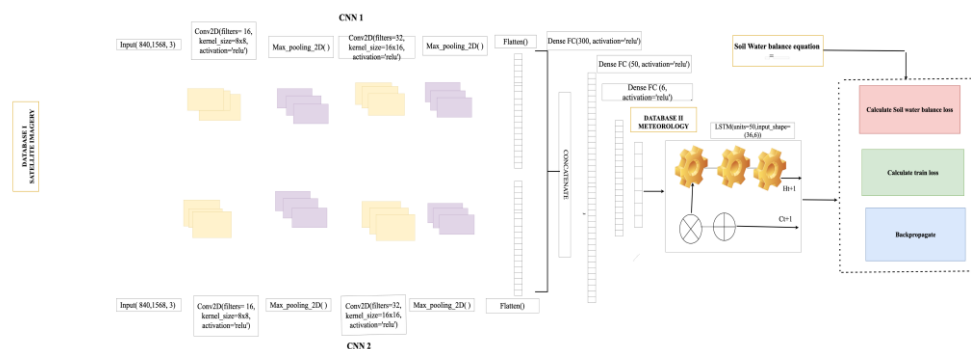


Figure 7 - Generic layout of proposed HDL informed CNN-LSTM model.

HDL: Hydrology Defined Loss

Soil moisture budgets from rainfall and evaporation have been studied by several researchers as an initial step in estimating the expected productivity of agricultural systems under various climatic conditions. These studies have also been used to develop alternative choices and decision strategies for the efficient use of limited available water. A realistic model differentiates between fallow and cropped conditions. The term "soil water balance" relates the moisture added through precipitation and/or irrigation to that lost through evapotranspiration, runoff and drainage. [Slatyer, 1967].

Evapotranspiration from a cropped area includes both soil evaporation and plant transpiration. Soil evaporation in a cropped area differs from that in fallow land. During the early stages of crop growth, evaporation is the primary source of moisture loss. However, as the crop progresses to the rapid vegetative growth and flowering/reproductive stages, transpiration becomes the dominant factor.

Crop Referenced Evapotranspiration: Penman Motheith

$$ET_c = \frac{.408(R_n - G) + \gamma \frac{900}{T + 273} \mu_2 (e_s - e_a)}{\gamma(1 + 34\mu_2)} \quad (2)$$

Where,

R_n = Net radiation at the crop surface

G = Soil heat flux density

T = Mean daily air temperature ($^{\circ}\text{C}$)

μ_2 = Wind speed at 2 meters height

e_s = Saturation vapor pressure

e_a = Actual vapour pressure

Δ = Slope of the vapour pressure curve

γ = Psychrometric constant

Runoff (R) - SCS Curve Number Method

$$Q = \frac{(P-.2S)^2}{(P+.8S)} \quad (3)$$

Where

R = Runoff

P = Precipitation

S = Potential maximum soil moisture retention after runoff begins

Physics penalty-based network weighing OR Observations about the loss function (HDL)

Crop water consumption, or evapotranspiration, represents the largest removal of water from the root zone, while precipitation and irrigation constitute the primary sources of water input. In the present study, PDNN models embeds the key variables involved in SWB phenomena to improve the prediction of crop yield. Knowledge of ET_c , precipitation, and the rainwater run-off are regressed along with the primary regression variable i.e., rice yield. The entire SWB can be capsulated by the \tilde{N} WY. The hybrid model, which uses physical principles as a guide, is more advantageous than both purely physical process models and pure machine learning models. This indicates that incorporating extracted physical rules into the form of loss functions can enhance predictive power.

Given the hidden representation $l_{i,t}^q$, of the LSTM cell on respective date q, the PDNN predicts the physical variables ET_c , P and R along-with the yield using the function transformation $p_{i,t}^{\sim d} = f(l_{i,t}^d)$

Where p^{\sim} represents the predicted values of [ET_c , P, R, Yield] on the date d and $f(.)$ can be implemented as fully connected network. By applying the model we compare predicted p^{\sim} and actual values in each year :

$$Diff_{i,t} = \sum_n \| l_{i,t}^n p^{\sim} - l_{i,t}^n p \| \quad (4)$$

We also consider a penalty for violating the SWB , as follows:

$$SWB_{i,t} = \sum_n (WY - P - ET_c + R) \quad (5)$$

We then combine Diff and SWB to define a physics based (cdl) loss .

$$loss_{hdl} = \gamma_1 \sum_{(i,t)} Diff_{i,t} + \gamma_2 \sum_{(i,t)} SWB_{i,t} \quad (6)$$

where γ_1 and γ_2 are model hyper-parameters.

At the end, we optimise the model combining the supervised loss and physical loss.

$$loss = loss_{RMSE} + loss_{phy} \quad (7)$$

2.4 Performance metrics

The model performance is the subjective aspect related to the problem at hand. For the purpose of regressing or forecasting the yield value, the focus is to identify the ML model that brings the right trade-off between the ability to assess the outliers and ability to output near real times values. The metrics employed are Root Mean Square Error (RMSE), Mean Absolute Error (MAE) and Mean Absolute Percentage Error (MAPE), the three metrics in Equations (6)–(8).

$$RMSE = \sqrt{\frac{1}{n} \sum_{i=1}^n (y_i^{\wedge} - y_i)^2} \quad (8)$$

$$MAE = \frac{1}{N} \sum_{i=1}^N |y_i - y_i^{\wedge}| \quad (9)$$

$$MAPE = \frac{100\%}{n} \sum_{i=1}^n \left| \frac{y_i - y_i^{\wedge}}{y_i} \right| \quad (10)$$

Where y_i = predicted value and y_i^{\wedge} = actual value

RESULTS

Experimental set up

The experiments carried out in this study (regression of yield estimation) were built on the top of deep learning framework of Tensorflow2019b and were executed on a server with Intel(R) Core (TM) i7-6850K processor with 64 Gb RAM and 2 GPUs (GeForce RTX 2080 Ti 11GB and GeForce GTX 1080 Ti 11GB) for parallel processing.

The input data consists of $m \times n$ patches with $p \times p$ size where m and n are the numbers in the spectral and temporal dimension respectively, and p is the patch size with the same width and height. In our case, the number of spectral bands is 10 and the temporal dimension is 2. In the initial experiments, patch size (p) is set to 21×21 and is fine-tuned later along with the other hyperparameters.

Hyperparameter tuning

Parameters such as the number of filters in the convolutional layer, the size and stride of the convolutional kernel, and the number of hidden cells in the LSTM layer are optimised using the random search method (Table 6). The optimisation of these hyperparameters spans numerous levels, leading to a computationally demanding and time-intensive task. This is due to the vast number of experiments generated by the combination of these hyperparameters.

For the selection of activation functions for the convolutional and LSTM layers, batch size, learning rate, and epochs, the grid search methodology is employed following conventional practices. An ablation study is also conducted to explore the impact of changing hyperparameters, and the results are depicted in Figure 8 .Four activation functions were explored for our proposed model, and among them, “relu” performs better for the CNN layers and “sigmoid” performs better for the LSTM layers (see Figure 9). The optimal hyperparameters selected for model training are outlined below.

Table 6 - Parameter setting for the CNN-LSTM architecture.

Parameters	Values
Convolutional layer filters	20
Convolutional kernel size	5
Convolutional kernel stride	3
Convolutional layer activation function	ReLU
Convolutional layer padding	Causal
Number of LSTM hidden cells	12
Number of skip connections	2
LSTM activation function	Sigmoid
Batch size	18
Loss function	Categorical cross entropy
Learning rate	0.0001
Epochs	40

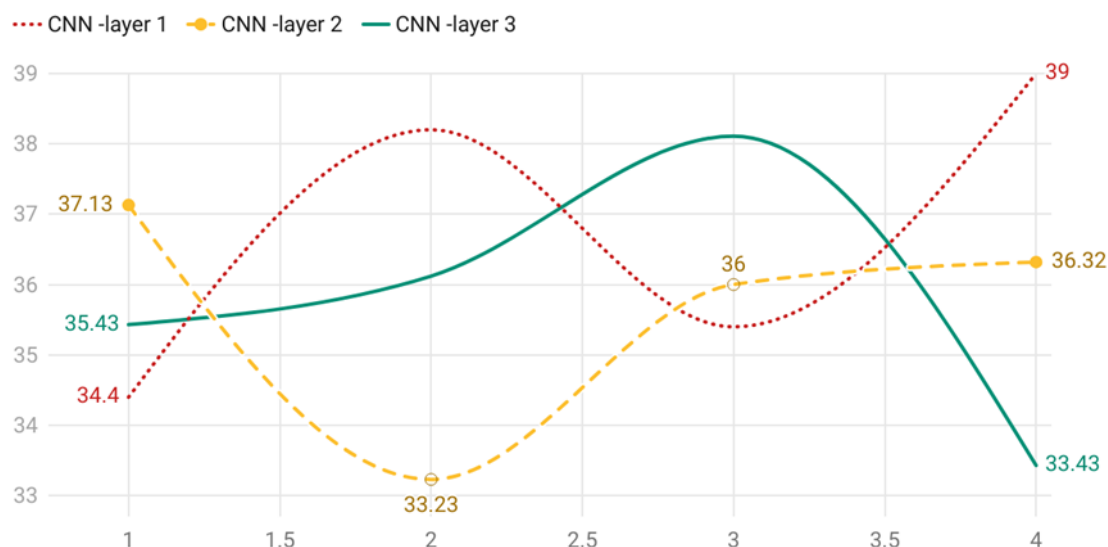


Figure 8- RMSE versus nth layer of CNN

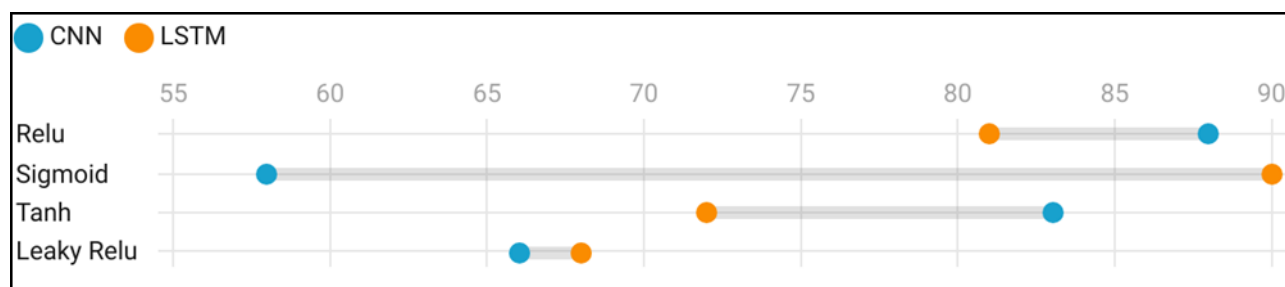


Figure 9 -Performance (validation accuracy %) of different activation functions for the LSTM and CNN.

Experimental Design

1. Can the proposed method outperform the other models?

The proposed method is compared with several baseline approaches using different testing years. Table 1 depicts proposed model outperforms other methods by decent margin in all the performance metrics. The CNN-LSTM model demonstrated significant potential for accurately predicting rice yield, leveraging both spatial (CNN) and temporal (LSTM) components of input data. The integration of the novel loss function, inspired by the soil water balance equation, provided domain-specific guidance for the optimization process, leading to enhanced model performance compared to conventional approaches. CNN performs worse amongst all as it does not consider physical loss term and temporal data shift across all the years. CNN_{PD} suffers from non-temporal learning. Integrated CNN-LSTM depicts weak regression ability due to pure supervised machine learning approach.

Table 7 – Performance comparison of models for the time period 2014-19.

Model	RMSE	MAPE	MAE	NSE
PDNN	.330	.370	.341	.330
CNN-LSTM	.361	.351	.351	.361
CNN_{PD}	.378	.378	.371	.378
$LSTM_{PD}$.363	.363	.350	.363

CNN	.384	.384	.401	.432
LSTM	.382	.382	.420	.401
GRU	.378	.378	.371	.378
GRU_{PD}	.363	.363	.350	.363

2. PDNN Performance evaluation as per water table statistics.

SWB \propto Water table depth

Rice Yield \propto Water table depth

Our actual water table depth values are available biannually for the months of May , August and Nov for 2014 [source: <https://www.cgwb.gov.in>]. Henceforth, prediction efficiency of model could be analysed for early season and end of season rice yield predictions.

The performance analysis of the PDNN model was conducted, and the findings were closely aligned with the water depth statistics for the respective blocks (Table 9). For the year 2014 in the Marh region, the PDNN model yielded a prediction with an RMSE of 0.345, compared to the CNN-LSTM model's RMSE of 0.372. in Suchetgarh, with a water depth of 2 meters during the dry season , the PDNN model demonstrated 3.2% better performance than the CNN-LSTM model. For some irrigated rice fields in bishnah, with a low water depth of 3 meters, the PDNN model's RMSE was slightly higher at 0.362, as the dataset did not account for irrigation practices. The evapotranspiration variable, influenced by soil moisture in the water balance equation of the PDNN model, helped improve network performance. Marh experienced a low water table, accompanied by heavy rains and a high runoff coefficient. The PDNN model accounted for these factors, resulting in an RMSE of 3.214.

Table 8

Metric	RMSE				MAE				SMAPE			
Year	2014	2015	2016	2017	2014	2015	2016	2017	2014	2015	2016	2017
Marh	0.44	0.51	0.48	0.38	0.46	0.52	0.50	0.51	0.47	0.51	0.51	0.51
Suchet Garh	0.42	0.47	0.50	0.42	0.45	0.50	0.42	0.47	0.45	0.50	0.47	0.47
Bishnah	0.36	0.41	0.42	0.48	0.38	0.40	0.41	0.41	0.42	0.46	0.44	0.41

Table 9. Statistics of water depth for the blocks of Jammu district for the year 2014.

(source: <https://www.cgwb.gov.in>).

Block	May	August	Nov
Marh	2.39	1.79	2.18
Suchet Garh	2.64	1.71	1.61
Bishnah	2.66	1.83	2.12

3. PDNN performance as per time scale of prediction with varying prediction lengths.

The discussed table 10 shows the results of the metrics in MSE and MAE of different deep learning models: CNN with HDL, LSTM with HDL and CNN-LSTM with HDL for all seasons and different forecast horizons. The dataset covers the early, middle, and late phases of a season with evaluation periods of 1, 3, and 5.

	Model	PDNN		CNN_{HDL}		$LSTM_{HDL}$		$(CNN - LSTM)_{HDL}$	
		MSE	MAE	MSE	MAE	MSE	MAE	MSE	MAE
Data set	Prediction length	.378	.378	.371	.378	3.08	3.24	4.02	.432
Early season	1	.363	.363	.350	.363	.458	3.58	2.58	.401
	3	.384	.384	.401	.432	13.21	17.21	15.21	.378
	5	.382	.382	.420	.401	3.70	6.40	3.40	.363
Mid season	1	.378	.378	.371	.378	0.42	0.45	0.38	0.45
	3	.363	.363	.350	.363	0.42	0.45	0.38	0.45
	5	.432	0.51	0.48	0.38	0.46	0.52	0.50	0.51
End of season	1	0.42	0.47	0.50	0.42	0.45	0.50	0.42	0.47
	3	0.38	0.45	0.46	0.34	0.42	0.45	0.38	0.45
	5	0.36	0.41	0.42	0.48	0.38	0.40	0.41	0.41

1. Model Comparison:

In contrast to other models, Hydrology Defined Neural Network continues to provide the best MSE and MAE results for the majority of forecast horizons and seasons. For example, at forecast horizon 1 during early season, it achieves MSE and MAE scores of 0.363 which is also better than the other models.

CNN with Hydrology Defined Loss has better, especially in the early season at forecast horizon 1, in 0.350 MSE and 0.363 MAE. However, he seems to make a lot more errors than the Hydrology Defined Neural Network in most situations.

The performance of LSTM with Hydrology Defined Loss is significantly low in comparison to others when looking at MSE and MAE, specifically in the case of longer predictions. For instance, at prediction length 5, the MSE is 3.70 for the early season, 0.46 for mid-season, and 0.38 at the end of season. The values for MAE are 6.40, 0.52, and 0.4 respectively which further suggests that LSTM does not perform well at higher prediction lengths.

CNN-LSTM acts just like LSTM but in a direction towards slightly better performance in certain situations, particularly in length 1 prediction. But as the prediction length keeps on growing, performance is decreasing, particularly in early season, in which MSE is 4.02 and MAE is 0.432 for length 5 prediction.

2. Seasonal Performance:

Early Season: Hydrology Defined Neural Network is the best performer overall across all the prediction lengths, most notably at prediction length 1. Other models such as CNN and LSTM have the errors rise as the prediction length rises, more particularly the LSTM and CNN-LSTM.

Mid Season: The relative performance difference between the models decreases. Hydrology Defined Neural Network is ahead, though, but relative competitive performance is exhibited by CNN with Hydrology Defined Loss and CNN-LSTM, particularly for prediction length 1.

End of Season: At this point, the models become more consistent in terms of their performance, with Hydrology Defined Neural Network still coming out on top in most cases. Surprisingly, the gap in model performance is more significant when increasing the prediction length, with LSTM models lagging behind, particularly in early season predictions.

3. Prediction Length Analysis

Prediction Length 1: Here, the models are best. The Hydrology Defined Neural Network has the lowest MSE and MAE in all seasons and hence ranks the highest for short-term predictions. CNN and CNN-LSTM are good here as well but take a backseat to the Hydrology Defined Neural Network.

Prediction Length 3: The performance deteriorates for longer prediction lengths. Hydrology Defined Neural Network remains the best, but CNN and LSTM models see an enormous rise in error.

Prediction Length 5: Here, performance is significantly lower for LSTM and CNN-LSTM models, particularly for early season predictions. Hydrology Defined Neural Network still fares well, but the performance decline for CNN-LSTM and LSTM models is noticeably clear, particularly for early season predictions (CNN-LSTM MSE of 4.02 and MAE of 0.432).

Comparative study with other research works.

CNN-LSTM	[Sun et al.]	CNN-LSTM	.353
CNN-LSTM	[Wang et al.]	CNN-LSTM	.361
CNN-LSTM	[Jiang et al.]	LSTM	.360
CNN-LSTM	[Sharma] et al.	CNN-LSTM	.358
CNN-LSTM	Proposed model	PDNN	.320

Proposed PDNN model outperforms highly recognized CNN and CNN-LSTM models for the task of crop yield forecasting. The gain (e.g., from 0.353 to 0.320) is quantitatively large, which means a superior ability to predict. The more general lower RMSE of PDNN across comparisons denotes integrating physics-based aspects holds a real benefit over purely data-based deep learning models.

CONCLUSION

This paper introduces a new Physics-Driven Deep Neural Network (PDNN) for predicting more precise crop yields, with particular emphasis on rice in Jammu district. Our method integrates a Soil Water Balance (SWB) equation framework into the CNN-LSTM deep learning model's loss function to offer domain-specific guidance (HDL) to improve spatio-temporal feature extraction. Experimental trials on real rice yield data from six blocks in Jammu district demonstrate that the PDNN is better predictable than several baseline models. The performance of PDNN was tested extensively against statistics of water table depth, an important factor driving both SWB and rice production. Model outputs always matched observed patterns of water depth. In Math (2014), for example, PDNN's 0.345 beat CNN-LSTM's 0.372. In Suchetgarh (2017 dry season, 2-meter water depth), the PDNN recorded a 3.2% improvement over CNN-LSTM. While R.S. Pura's irrigated fields with a low water depth of 3 meters accounted for a

slightly elevated RMSE (0.362) due to unexplained irrigation practices in the data, the evapotranspiration term of PDNN's water balance equation continued to contribute to improved network performance. The model might explain extreme conditions of high precipitation and large runoff coefficients, like in Bishnah (2016 low water table), with an RMSE of 3.214.

In addition, the PDNN performed best when it forecasted yields at the beginning of the season up to three time steps in advance, at which point the minimum RMSE was obtained. Such ability at early and accurate prediction is highly useful for forward-looking policy-making and farm management. In further pursuit, this study would explore inclusion of irrigation management data which will capture the soil moisture dynamic effectively.

REFERENCES

- [1] Michiel GJ Kallenberg, Bernardo Maestrini, Ron van Bree, Paul Ravensbergen, Christos Pylianidis, Frits van Evert, and Ioannis N Athanasiadis. Integrating processed-based models and machine learning for crop yield prediction. *arXiv preprint:2307.13466*, 2023
- [2] Han, J., Shi, L., Pylianidis, C., Yang, Q. and Athanasiadis, I.N., 2023. Deeporyza: a knowledge guided machine learning model for rice growth simulation. In *2nd AAAI Workshop on AI for Agriculture and Food Systems*.
- [3] Shahhosseini, M., Hu, G., Huber, I. and Archontoulis, S.V., 2021. Coupling machine learning and crop modeling improves crop yield prediction in the US Corn Belt. *Scientific reports*, 11(1), p.1606.
- [4] Christos Pylianidis, Val Snow, Hiske Overweg, Sjoukje Osinga, John Kean, and Ioannis N Athanasiadis. Simulation-assisted machine learning for operational digital twins. *Environmental Modelling & Software*, 148:105274, 2022.
- [5] Ryan F McCormick, Sandra K Truong, Jose Rotundo, Adam P Gaspar, Don Kyle, Fred Van Eeuwijk, and Carlos D Messina. Intercontinental prediction of soybean phenology via hybrid ensemble of knowledge-based and data-driven models. in *in silico Plants*, 3(1):diab004, 2021.
- [6] George Worrall, Anand Rangarajan, and Jasmeet Judge. Domain-guided machine learning for remotely sensed in-season crop growth estimation. *Remote Sensing*, 13(22):4605, 2021.
- [7] Xie, W., Kimura, M., Takaki, K., Asada, Y., Iida, T., & Jia, X. (2022). Interpretable framework of physics-guided neural network with attention mechanism: Simulating paddy field water temperature variations. *Water Resources Research*, 58, e2021WR030493.
- [8] He, E., Xie, Y., Liu, L., Chen, W., Jin, Z. and Jia, X., 2023, June. Physics guided neural networks for time-aware fairness: an application in crop yield prediction. In *Proceedings of the AAAI Conference on Artificial Intelligence* (Vol. 37, No. 12, pp. 14223-14231).
- [9] Salman, M., García-Vila, M., Fereres, E., Raes, D. and Steduto, P., 2021. *The Aqua Crop model—Enhancing crop water productivity: Ten years of development, dissemination and implementation 2009–2019* (Vol. 47). Food & Agriculture Org.
- [10] Maulana, F. (2023) Improving Potato Yield Estimation through Physics-Guided System Identification with Hybrid Approach .
- [11] Cuomo, S., Di Cola, V.S., Giampaolo, F., Rozza, G., Raissi, M. and Piccialli, F., 2022. Scientific machine learning through physics-informed neural networks: Where we are and what's next. *Journal of Scientific Computing*, 92(3), p.88.
- [12] <https://jammu.nic.in/blocks/>
- [13] Irrgang, Christopher, Niklas Boers, Maike Sonnewald, Elizabeth A. Barnes, Christopher Kadow, Joanna Staneva, and Jan Saynisch-Wagner. "Towards neural Earth system modelling by integrating artificial intelligence in Earth system science." *Nature Machine Intelligence* 3, no. 8 (2021): 667-674
- [14] Willard, Jared, Xiaowei Jia, Shaoming Xu, Michael Steinbach, and Vipin Kumar. "Integrating physics-based modeling with machine learning: A survey." *arXiv preprint arXiv:2003.049191*, no. 1 (2020): 1-34.
- [15] Raissi, Maziar, Paris Perdikaris, and George E. Karniadakis. "Physics-informed neural networks: A deep learning framework for solving forward and inverse problems involving nonlinear partial differential equations." *Journal of Computational physics* 378 (2019): 686-707.
- [16] <https://cgwb.gov.in/cgwbpmn/>

- [17] Zhao, Wen Li, Pierre Gentine, Markus Reichstein, Yao Zhang, Sha Zhou, Yeqiang Wen, Changjie Lin, Xi Li, and Guo Yu Qiu. "Physics-constrained machine learning of evapotranspiration." *Geophysical Research Letters* 46, no. 24 (2019): 14496-14507.
- [18] Liu,Y.;Zhang,S.;Zhang,J.; Tang, L.; Bai, Y. Using Artificial Neural Network Algorithm and Remote Sensing Vegetation Index Improves the Accuracy of the Penman-Monteith Equation to Estimate Cropland Evapotranspiration. *Appl. Sci.* **2021**, *11*,8649. <https://doi.org/10.3390/app11188649>
- [19] Liang, J., Li, W., Bradford, S.A. and Šimůnek, J., 2019. Physics-informed data-driven models to predict surface runoff water quantity and quality in agricultural fields. *Water*, *11*(2), p.200.
- [20] Ishaan Seshukumar Pothapragada, Sujatha R,GANs for data augmentation with stacked CNN models and XAI for interpretable maize yield prediction,Smart Agricultural Technology,Volume 11,2025,100992, ISSN 2772-3755.
- [21] WangY,ZhangZ,FengL,DuQ,RungeT(2020)Combining multi-source data and machine learning approaches to predict winter wheat yield in the conterminous united states. *Remote Sensing* 12(8):1232 .
- [22] Sun J, Di L, Sun Z, Shen Y, Lai Z (2019) County- level soybean yield prediction using deep ^[11]_{SEP}CNN-LSTM model. *Sensors* 19(20):4363
- [23] Jiang, H., Hu, H., Zhong, R., Xu, J., Xu, J., Huang, J., ... & Lin, T. (2020). A deep learning approach to conflating heterogeneous geospatial data for corn yield estimation: A case study of the US Corn Belt at the county level. *Global change biology*, *26*(3), 1754-1766.
- [24] Slatyer, R. O. "Internal water relations of higher plants." *Annual Review of Plant Physiology* 13.1 (1962): 351-378.